Ann Vasc Dis Vol. 16, No. 3; 2023; pp 155–162

Online August 4, 2023
doi: 10.3400/avd.oa.23-00045

Original Article

Study on an Onset Mechanism of MDRPU by Wearing Elastic Stockings: Numerical Simulation by Two-Dimensional Mechanical Model

Kokichi Hashimoto, MEng, Ayako Tosaki, BEd, LMT, and Nanae Matsuda, BLA, LMT

As compared with pressure injuries, the mechanism the development of medical device related pressure ulcers (MDRPU) is not revealed enough. According to studies on severity and frequent site of occurrence, MDRPUs are surmised to occur the surface of the skin. In this study, we assess theoretical and experimental analysis by two-dimensional mechanical model for elastic stockings (ES) wear the lower limbs with or without dug into the skin by the wrinkles and curling up of ES. The Finite Element Method (FEM) was used to calculate the stress on the skin and subcutaneous tissue, because of elucidating the mechanism of MDRPU. The FEM used a triple-layered cylindrical model simulating the skin, subcutaneous tissue, and bone. Regarding the interface pressure (compression pressure), two samples were created: the one is applying a uniform pressure of 5.3 kPa on the skin surface simulating the correct wearing of ES, and the other is applying a pressure of 16 kPa on the part of the skin on which ES dug in. The results were as follows: the internal stress on the skin and subcutaneous tissue was maximum at the site where ES dug in, producing stresses of 54 kPa, 50 kPa, and 21 kPa in the circumferential, longitudinal, and radial directions, respectively. The uniform pressure produced an internal stress of 5–9 kPa on the skin surface. Unlike the mechanism of pressure injury formation, we considered compressive strength from tensile of the circumferential and longitudinal directions, furthermore the additive radial pressure at the digging site on the skin due to the wrinkles and curling of ES, which is one of the factor to cause strong external force in the MDRPU formation. (This is secondary publication from Jpn J Phlebol 2021; 32(1): 119–126.)

Keywords: medical device related pressure ulcers, elastic stockings, Finite Element Method, stress in skin and subcutaneous tissue

Higashikanagawa Tosaki Acupuncture Clinic, Yokohama, Kanagawa, Japan

Received: June 5, 2023; Accepted: June 24, 2023

Corresponding author: Kokichi Hashimoto, MEng. Higashikanagawa Tosaki Acupuncture Clinic, 1-20-1-602 Nishikanagawa, Kanagawa-ku, Yokohama, Kanagawa 221-0822, Japan
Tel: +81-45-431-0706, Fax: N/A
E-mail: khashi39@jcom.zaq.ne.jp

This is secondary publication from Jpn J Phlebol 2021; 32(1): 119–126.

Introduction

A medical device-related pressure ulcer (MDRPU) is an injury to the skin and subcutaneous tissue caused by the pressure of a diagnostic or therapeutic medical device. It is distinct from conventional pressure injuries, that is, self-weight-related pressure ulcers. However, MDRPUs and conventional pressure injuries are both pressure injuries and fall into the pressure ulcer category. Although there are some similarities between pressure injuries and MDRPUs in that they are wounds caused by local external forces, it has been reported that pressure ulcers are almost entirely caused by body weight, whereas MDRPU is not always related to weight.[1,2] According to a report,[3] based on a survey of general hospitals and university hospitals, MDRPUs are distinguished by the common sites, which are often on the foot or lower extremity, and the medical device used, which is often elastic stockings (ES). In terms of severity (depth) of pressure injuries, 14% were erythematous (redness), 48% extended up to the dermis, and 23% were from the subcutaneous tissue to the joint cavity or body cavity, in comparison with 33%, 40%, and 11% in MDRPU, respectively.[3,4] Differences in depth ranges were observed between pressure injuries and MDRPUs.

To elucidate the mechanisms of pressure injury development, various studies, including case studies, have been conducted, with the results leading to the development of evidence-based guidelines (Pressure Injury Prevention and

Management Guidelines, 4th Edition; Journal of the Pressure Injury Society, 2015) and other measures required to prevent pressure injury development. To investigate the mechanism of pressure injury development, various numerical approaches using the finite element method (FEM), a numerical analysis method in which an object is divided into elements of finite size and modeled as a collection of elements,[5] have been attempted, including two-dimensional modeling of the buttocks, detailed analysis using MRI image information as boundary conditions of the FEM, and modeling the process of pressure injury development.[6–10] Nevertheless, research on pressure ulcer development in MDRPUs has been insufficient. In the case of ES for venous thromboembolism prevention, "Prevention and Management of MDRPU"[1] states that common sites of MDRPUs include areas with soft skin, as well as with protruding or movable parts and joints of bones. The wrinkling and curling up of ES, and the pressure of ES on protruding areas are potential factors in the occurrence of MDRPUs. Additionally, when we compare the severity (depth) of pressure injuries with the location of MDRPUs caused by ES, we can assume that MDRPU wounds are shallower and occur closer to the skin.

Our clinic was established to provide conservative treatment for patients with lymphedema. Initially, compression therapy was administered during the intensive drainage phase using elastic bandages as recommended by the International Society of Lymphology. However, due to the difficulty of patients continuing compression therapy on their own, we have been working with the use of ES, which are easier to manipulate and provide more stable compression pressure than bandages, in the intensive drainage phase.[11–14] In actual clinical practice, transient redness prior to wounding can be seen on the skin by wrinkling and curling up of ES. Thus, it was believed that by understanding and applying the mechanism of wound development specific to ES, more effective ES and practice preventive care that considers MDRPU could be selected and prepared. By contrast, numerical analysis of a lower extremity model on an improvement in sclerosis of the skin by wearing a garment showed that compression pressure by a garment had little effect on the lower subcutaneous tissue.[15] In this study, we hypothesized that MDRPU originates from the superficial layers of the skin. For verification purposes, we assumed that the wrinkles and curling up that occur during the wearing of ES, one of the medical-related devices, dig into the skin, which causes MDRPUs. We replaced them with a two-dimensional linear elasticity model that comprises a three-layer structure that mimics the lower limb and calculated the stress on the skin and subcutaneous tissue using an FEM-based numerical analysis to elucidate the mechanism.

Materials and Methods

One of the most common sites and characteristics of pressure injuries induced by ES is wrinkling and curling up, which is caused by the upper edge or movement of ES in soft skin areas other than joints and hard tissues such as bones. To evaluate the digging into skin caused by compression pressure, wrinkling, and curling up by ES, we replaced those with a two-dimensional linear elastic model simulating the lower limb and calculated the stress (a force acting per unit area) on the skin and subcutaneous tissue by using the FEM. The model was axisymmetric and defined using a cylindrical coordinate system (R, θ, Z). The stress components in the tissue were the circumferential stress (hoop stress) $\sigma\theta$ acting tangentially to the circumference, the longitudinal (Z-direction) stress σz, and the radial (R-direction) stress σR, which is perpendicular to the skin (**Fig. 1**). The FEM modeling comprised a three-layered structure: a cylinder of 40-mm radius and 200-mm length; a conical hard tissue (bone) with radiuses of 30 and 12 mm at the upper and lower ends, respectively; and two layers of soft tissue (skin and subcutaneous tissue) covering the surface. The skin was uniformly 2 mm thick on all surfaces, and the subcutaneous tissue thickness varied longitudinally depending on the diameter of the hard tissue, allowing changes in the stress in the tissue due to compression pressure and digging into the skin by ES (**Fig. 2**).

In terms of the interface pressure (compression pressure) by ES, two models were created: one applying a uniform pressure of 40 mmHg (5.3 kPa) to the skin surface simulating the correct wearing of ES (flat model) and the other assuming a ring-shaped digging into the skin due to the curling up of ES at two locations (thick arrow in **Fig. 2**: between 15 and 20 mm at the A–A′ portion and

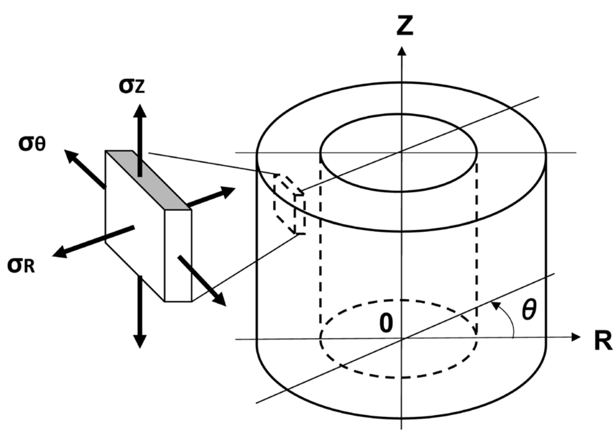

Fig. 1 Cylindrical coordinate system (R, θ, Z) and three stress components (radial stress σR, circumferential stress σθ and longitudinal stress σz) for simulation modeling.

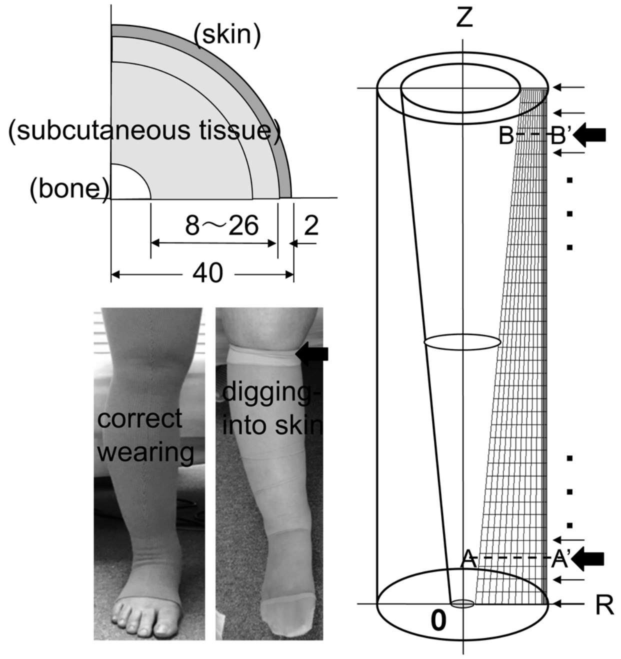

Fig. 2 Simulation model for the lower limb (2-dimensional Finite Element Model with rectangular elements): A triple-layered cylindrical structure (skin, subcutaneous tissue, and bone) with 40 mm in outer radius and 200 mm in length. The diameters of the upper and lower ends of the bone are 30 mm and 12 mm, respectively, and the skin has a uniform thickness of 2 mm. Two interface pressure (compression pressure) models were created: one applying a uniform pressure of 40 mmHg (5.3 kPa) on the skin surface simulating the correct wearing of ES (Flat Model), and the other applying a pressure of 120 mmHg (16 kPa) on the part of the skin on which ES dug in (Digging-into Model). Two bold arrows in the figure indicate the site of ES digging into the skin. The image on the left shows a correctly-worn ES, and on the right shows curling-up of ES digging into the skin.

between 180 and 185 mm at the B–B′) with different longitudinal subcutaneous tissue thickness in the flat model (digging into the model). The thickness of the subcutaneous tissue in the digging-into area is 24.425 mm in the A–A′ area and 9.575 mm in the B–B′ area. The area with the greatest subcutaneous tissue thickness was assumed to be the thigh/leg area, and the area with the least thickness was assumed to be the knee joint/ankle joint area. At the digging-into area, the model was subjected to a pressure of 120 mmHg (16 kPa), which was three times the uniform pressure of the flat model. Using the measurement data from a collaborative study, the uniform compression pressure acting on the model was set to 40 mmHg based on the measured value at point F on the thigh of the pressure gradient from peripheral to central during the transition from the intensive drainage phase to the maintenance phase.[13] By referencing the pressure during the two superimposed stockings, the pressure of the digging-into model was determined. The effect of wearing two superimposed stockings in patients with lymphedema (increase in pressure when wearing two layers of stockings compared to the pressure with the first layer) was found to be 1.2–1.7 times greater in a collaborative study[13] or 1.7–1.9 times greater in healthy subjects as reported by Hirai et al.[16] and Partsch et al.[17] Based on the above values, the pressure of digging into the skin was determined to be greater than that of two superimposed stockings and was set to be three times the uniform wearing pressure of the flat model.

Physical properties such as bone (Young's modulus, 17,000 kPa), skin (850 kPa for age 30 years and older), subcutaneous fat (182 kPa), and muscle (36 kPa for rectus femoris) were taken from the "RIKEN Mechanical Property Database."[18] The Young's modulus of subcutaneous tissue used in the model was calculated synthetically, with the assumption that subcutaneous fat and muscle were connected in series, and set to 30 kPa. The Poisson's ratio was 0.45 for skin and 0.49 for subcutaneous tissue. The hard tissue was assumed to be rigid compared to Young's modulus of the skin and subcutaneous tissue. The FEM has 560 elements (rectangular elements), 1,789 nodes, and 137 constraint nodes. The three stresses, σθ, σz, and σR, were evaluated for each model, along with the shear stress τRZ occurring in the R–Z cross-section for the digging-into model. Moreover, the stress σmises based on Von Mises' fracture theory, which applies to ductile materials and states that an object fails when its internal stress reaches its own strength was evaluated. FEM software A3H (for two-dimensional structural analysis) and C10H (for FEM cross-section data generation) (Sanseikai, Mie Prefecture, Japan) were used.

Results

Unless otherwise specified, stresses (in kPa) are compressive stresses, and values in graphs and figures are distinguished from tensile stresses, with compression as the negative sign. Von Mises stress (σmises) is a magnitude-only quantity with no direction.

Skin surface displacement: The radial change in the skin surface ΔR from before wearing ES (ΔR = 0) due to compression was 0.16 mm in the A–A′ area and 0.08 mm in the B–B′ area for the flat model. It was almost proportional to the subcutaneous tissue thickness. By contrast, the digging-into model was 1.03 mm for the A–A′ area and 0.63 mm for the B–B′ area (**Fig. 3** shows ΔR). The longitudinal change (ΔZ) ranged from 0 to 0.03 mm for the flat model and from 0.17 to 0.09 mm for the digging-into model.

Stress distribution in the cross-section of the digging-into portion: The stress distribution in the cross-section showed similar patterns in the A–A′ and B–B′ areas. In the

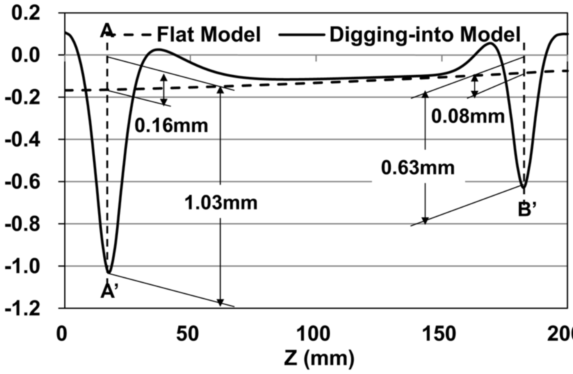

Fig. 3 Radial displacement (ΔR) relative to skin surface corresponding to Z direction.

A–A′ area (**Fig. 4(1)**), the stresses σθ, σz, and σR (hereinafter referred to as the three stresses) ranged from 7 to 10 kPa in the subcutaneous tissue layer. The maximum compressive stress of σθ was 53.5 kPa at the skin surface. By contrast, σz became tensile near the boundary between the subcutaneous tissue and skin layer, with a maximum tensile stress of 10.4 kPa at the lowest skin layer and a maximum compressive stress of 49.7 kPa at the skin surface. σR showed a maximum compressive stress of 20.6 kPa at the skin surface. In the B–B′ area (Figure omitted), the three stresses at the skin surface were 41.6, 42.2, and 20.6 kPa, respectively. In the A–A′ area of the flat model (**Fig. 4(2)**), the three stresses in the subcutaneous tissue layer were almost uniform at 5 kPa, and the three stresses at the skin surface were 8.7, 6.3, and 5.3 kPa, respectively. The distribution of the three stresses at and around the A–A′ area of the digging-into model has been visualized in **Fig. 5** (σθ, σz, and σR in **Fig. 5**). σθ and σz show the maximum compressive stress at the skin surface, and σz shows the tensile stress at the lowest skin layer. At the boundary with the element adjacent to the digging-into area, the shear stress τRZ was maximum at 11 kPa at the skin layer and 2.5 kPa at the skin surface (**Fig. 4(3)**).

Von Mises stress (σmises) distributions: The σmises distribution of digging-into model in and near the A–A′ area was visualized (σmises in **Fig. 5**). The σmises distributions in the A–A′ area's skin layer and the lowest layer of subcutaneous tissue were 26–33 kPa and 0.4 kPa, respectively, and for the B–B′ area, 16–25 kPa and 0.7 kPa, respectively (**Fig. 6**). The σmises distributions of the flat model, the skin layers in the A–A′ and B–B′ areas were 3.0–3.3 and 1.3–1.4 kPa, respectively, and the subcutaneous tissue layer was 0.21 kPa in both areas.

Stress distribution on the skin surface and lowest layer of subcutaneous tissue in the longitudinal direction of digging-into model: On the skin surface (**Fig. 7(1)**), the three stresses turned to the tensile from the compressive side in front and behind the digging-into skin position:

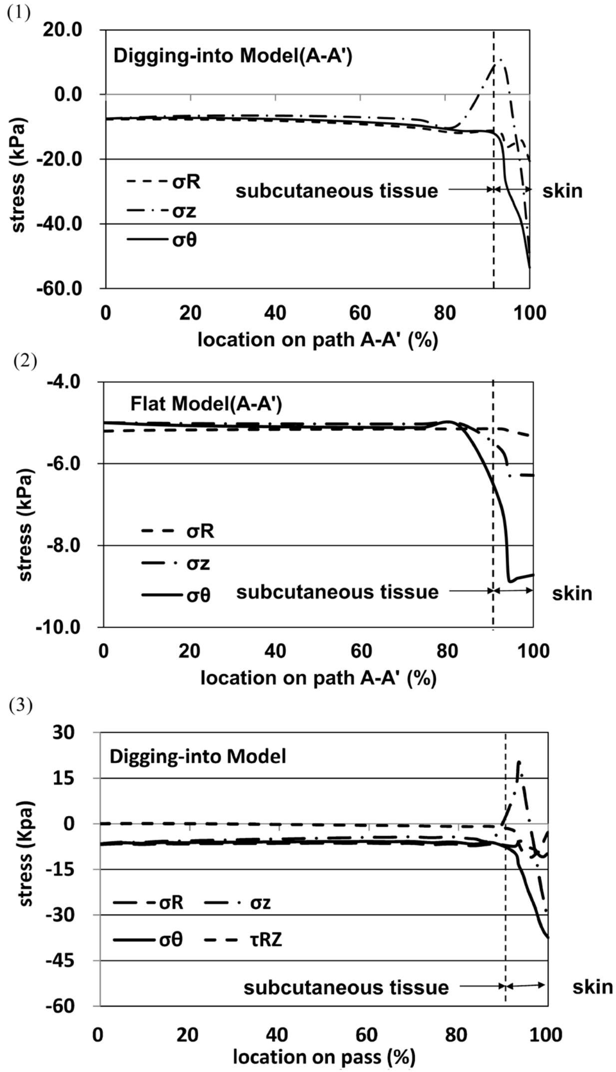

Fig. 4 (**1**) Stress distributions of three components (σθ, σz, σR) on the cross section A–A′, in Digging-into Model. The negative sign of stress (kPa) represents compressive stress. (**2**) Stress distributions of three components on the cross section A–A′, in Flat Model. (**3**) Stress distributions of components (σθ, σz, σR, τRZ) in the vicinity of cross section A–A′, in the Digging-into Model. τRZ is a shear stress on the R–Z plane in the cylindrical coordinate system.

σθ>σz>σR in the A–A′ area and σθ≈σz>σR in the B–B′ area. Except for the digging-into area, the σR was almost uniformly 5 kPa in all regions and 20.6 kPa in the digging-into area, which ranged from 40% (A–A′) to 50% (B–B′) of σθ (**Figs. 7(1)A** and **7(1)B**). By contrast, in the lowest layer of the subcutaneous tissue (**Fig. 7(2)**), the three stresses in each area were almost equal in both the A–A′ and B–B′ areas, but unlike the skin surface, the B–B′ area (10.9–11.4 kPa) showed greater stress than that in the A–A′ area (7.4–7.7 kPa) (**Figs. 7(2)A** and **7(2)B**).

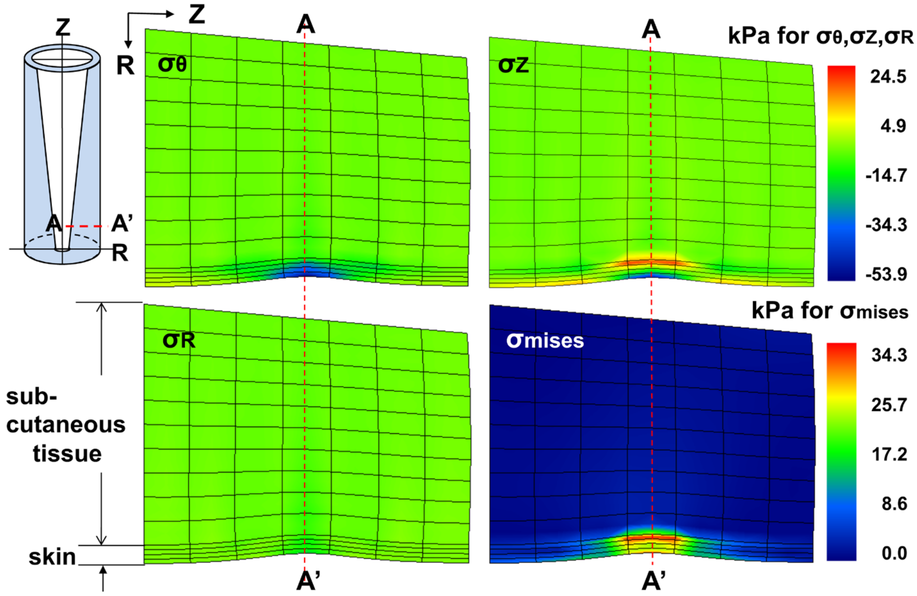

Fig. 5 Stress distributions of three components and Von Mises stress (σmises) on the cross section A–A′ in Digging-into Model by contour map.

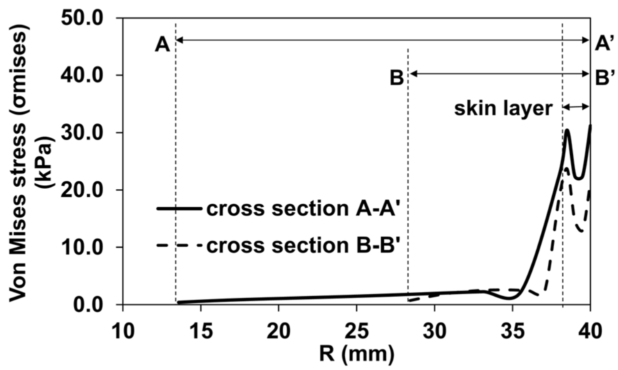

Fig. 6 Distributions of Von Mises stress (σmises) on the cross section of A–A′ and of B–B′.

Discussion

Because the pathway of the load transmitted to the skin and subcutaneous tissue differs in this study between the pressure injury that is likely to occur near the bony prominences due to own weight and compression pressure, a mechanical model for numerical analysis should be developed, considering the load pathway and whether the affected area is locally or entirely. The modeling by ES was developed with the following in mind. The Young–Laplace equation in physics relates the pressure difference between two phases at an interface with curvature to the surface tension and curvature of the interface, and Laplace's law uses this equation to predict the interface pressure (compression pressure) P (mmHg, Pa) of an elastic garment.[19] According to this law, the compression pressure generated by an elastic garment is proportional to the garment's tension and inversely proportional to the limb's circumference. Tension is a force that acts tangentially around the circumference of the limb, causing strain or stress on the skin and subcutaneous tissue. The modeling in this study was inspired by Laplace's law and the stress analysis of thin-walled cylinders subjected to internal pressure in the mechanics of materials. When a high-pressure fluid flows through a tube (thin-walled cylinder) whose thickness (wall thickness) is smaller than its diameter, the circumferential stress σθ acting on the cylinder tangentially to the circumference and the tensile stress σz in the longitudinal direction both play important roles in the tube's strength.[20] A lower limb wearing ES can be modeled as a cylinder composed of a thin skin layer and subcutaneous tissue (approximately 1/30th of the skin in terms of Young's modulus, which is an index of the material's resistance to deformation or resistance and stiffness), which is softer than the skin on the inside, as well as bone in the center, which is considered rigid. This can be modeled as a cylinder with a cylindrical coordinate system (R, θ, Z) that is subjected to external pressure (compression pressure by ES). We previously reported the results of FEM analysis on the improvement of skin stiffness when a corrugated urethane garment was applied to a lower limb with lymphedema.[15] This study attempted to apply this report by modeling the garment as a two-dimensional axisymmetric linear elastic body in a cylindrical coordinate system.

Numerical analysis using mechanical models provides information on mechanical states such as stress and strain that extend from the skin to the subcutaneous tissue. However, experimental studies are often required to explain how these conditions ultimately lead to tissue dam-

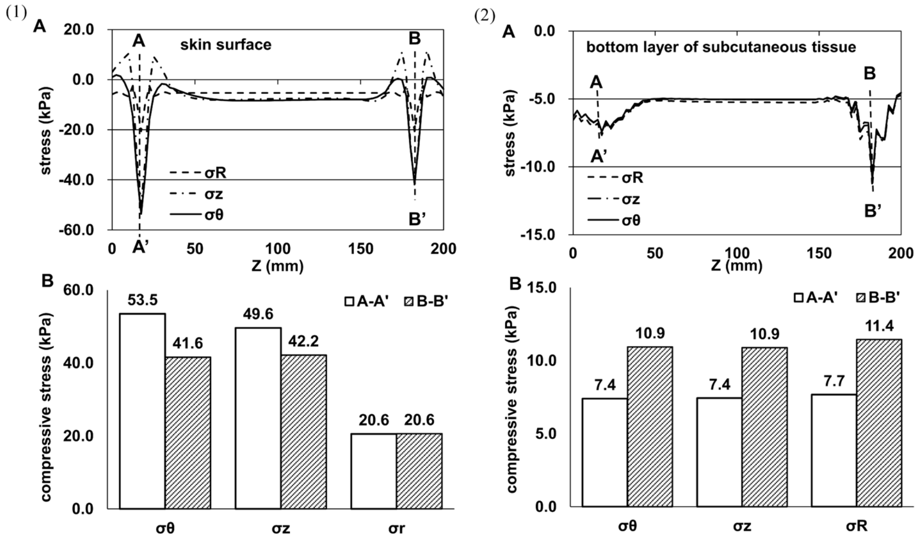

Fig. 7 (**1**) Stress distributions of three components on skin surface (**A**), and the comparison of three stresses between the cross section of A–A′ and of B–B′ (**B**), in Digging-into Model. (**2**) Stress distributions of three components on bottom layer of subcutaneous tissue (**A**), and the comparison of three stresses between the cross section of A–A′ and of B–B′ (**B**), in Digging-into Model.

age. There have been many studies of mechanical loading influencing tissue damage and the relationship between loading and blood flow in the context of pressure injuries. Regarding the surface loading and skin capillaries at the skin, Bader et al. demonstrated that if the mechanical stress fields are maintained for prolonged periods, tissue ischemia leads to cell necrosis based on experimental and numerical analysis of mechanical loading on the forearm skin surface.[21)] Bennett et al.,[22)] who measured the palm, Kayama et al.,[23)] and Shimizu et al.,[24)] who applied mechanical loading to the sacral bone region, all stated that compression forces besides shear forces are necessary for blood flow occlusion. Yamamoto et al. reported that a numerical analysis of cutaneous blood flow and compression pressure in the sacral bone region and their experimental results showed that the greater the pressure, the more the blood vessels were deformed or occluded, and the blood flow decreased.[25)] In terms of tissue deformation and ischemia in animal experiments, Stekelenburg et al. suggested that ischemia-related large deformations are a major factor in irreversible damage based on the mechanical loading through the indenter and tourniquet that causes ischemia.[26)] The above studies on blood flow alteration or tissue damage used nonuniform compression or shear forces to localized skin surface areas to elucidate the mechanism of pressure injury development. In this study, when ES is properly applied, the loading by the ES exerts only vertical force (compression pressure) on the skin surface, as indicated by Laplace's law, and tissue damage is unlikely to occur. By contrast, when nonuniform external pressure is applied due to digging into the skin by ES, the maximum compressive forces in the circumferential direction act tangentially to the circumference, and longitudinal direction on the skin surface. These forces are assumed to deform the tissue in the digging-into area just below the skin surface and reduce tissue blood flow and ischemia.

The interface pressure (compression pressure) of ES causes displacement relative to the skin surface in the radial direction (R-direction in **Fig. 1**) and longitudinal direction (Z-direction), resulting in changes in ΔR and ΔZ, respectively, in the tissue. As described in the displacement of the skin surface in the results, ΔZ is smaller than ΔR. Contrary to the flat model, which assumes that ES are correctly worn, the digging-into model provides 6–8 times the amount of change in the R-direction to the skin surface of the digging-into area (**Fig. 3**). This ring-shaped digging-into exerts significant stresses on the skin and subcutaneous tissue. Because the mechanical model in this study is axisymmetric, the stresses are theoretically the three stresses along with a shear stress component τRZ in the R–Z plane. In the flat model with correctly worn ES, τRZ does not occur. In the vicinity of the area of the digging-into model, the magnitude of shear stress in the skin layer and its surface is less compared to the three stresses ($\sigma\theta$, σz, and σR) and can be ignored in the subcutaneous tissue (**Fig. 4(3)**). However, according to Bennett et al.'s view,[22)] if the shear force is low and the compressive force is large, blood flow occlusion occurs. This raises an issue regarding future research on the shear force by the digging in of ES and blood flow.

To measure blood flow in studies of pressure injuries, Bennett et al. measured arteriolar blood flow[22)]; using the laser Doppler method, Bader et al.,[21] Kayama et al.,[23] Shimizu et al.,[24] and Yamamoto et al.[25] observed tissue blood flow, including capillaries immediately beneath the skin surface. The three stresses are greatest at the skin surface because of digging in by ES, whereas those at subcutaneous tissue are in the range of 7–10 kPa (**Fig. 4(1)**), indicating that the compression pressure by digging in has a minor effect. Although the loading form differs from that used in the study of pressure injuries, it is assumed that prolonged pressure from digging in by ES causes deformation and occlusion of blood vessel walls, thereby inhibiting blood flow. In other words, based on studies on mechanical loading and blood flow/ischemia, to clarify the mechanism of pressure injury development, as well as studies on tissue blood flow just beneath the skin surface, it is assumed that the digging into the skin due to wrinkling and curling up of ES causes large deformation of the skin layer, and mainly the circumferential stress $\sigma\theta$ acting tangentially to the circumference and longitudinal stress σz generate the compression stress and superimpose additional radial stress. Therefore, blood flow is impeded by deformation and occlusion of vessel walls in the skin layer, and these mechanisms are accountable for MDRPUs caused by ES.

Meanwhile, Von Mises stress (σmises) based on fracture theory was the highest in the skin layer, 33 kPa (σmises at A–A′ area in **Fig. 5**) for the digging-into model and 3.3 kPa for the flat model. When ES digs into the skin, in the skin layer, σmises was nearly twice as large as a pressure of 16 kPa on which ES dug in and 10 times larger than the uniform wearing pressure.

The analysis of the relationship between the stress due to digging in and the thickness of the subcutaneous tissue (cross-section of A–A′ and B–B′) revealed that σmises was greater in the A–A′ area, where the subcutaneous tissue was thick than in the B–B′ area (**Fig. 6**). The flat model showed the same trend. These results suggest that the skin layer due to digging in of ES tends to develop wounds in areas with thicker tissue thickness.

By contrast, the σmises at the bone boundary, that is, in the lowest subcutaneous tissue layer were smaller in the A–A′ area than in the B–B′ area (**Fig. 6**). This was also observed in the three stress components (**Fig. 7(2)B**). However, unlike the skin surface (**Fig. 7(1)B**), at the bottom of the layer of subcutaneous tissue, σR is slightly larger than $\sigma\theta$ and σz, and forces perpendicular to the skin act on the bottom of the layer the same as the circumferential and longitudinal directions. Our simple modeling suggests that if tissue thickness is small, including the case of pressure concentration by ES on the protruding parts such as bones and joints, compression pressure of ES not only causes wounding on the skin surface but also affects the bottom of the layer of the subcutaneous tissue due to forces perpendicular to the skin, which may cause wounding.

The mechanical model utilized in this investigation assumes no tissue boundary slippage. A skin tear is a traumatic wound caused by shearing and friction forces that separate the epidermis and dermis from the underlying structures, which primarily affects the extremities of elderly individuals.[27] Murasawa et al. applied continuous shear stress loading to porcine skin tissue and observed that elastic fibers located directly beneath the epidermal cells were destroyed, suggesting that they were the cause of skin damage.[28] Thus, when wearing ES with antislip protection, such as adhesive tape or silicone grips, if the ES is pulled too tightly or twisted, the restoring force of the ES exerts frictional and shear forces on the skin contact surface of the protection, resulting in damage to the superficial skin layer, which may be a cause of MDRPU. Conversely, skin thinning is often caused by the development of MDRPU due to ES[29] and also by bony prominences such as the tibia and fibula, which cause localized pressure when wearing ES.[1,29] Nevertheless, elucidating the mechanism of MDRPU development in the superficial skin layer of the skin remains a challenge. In this study, we focused on wrinkles and curling up, which are frequently observed in MDRPUs at the time of wearing of ES, in the hope that they will be useful in clinical practice.

Conclusion

While wearing the ES, the digging into the skin induced by the wrinkling and curling up of the ES causes significant deformation and compression forces on the skin. In other words, compared with uniform compression pressure with properly worn ES, digging into the skin of ES generates a large deformation of the skin layer, with circumferential and longitudinal stresses primarily causing compression stress and superimposing additional radial stress. In contrast to the mechanism of pressure injury development, the largest external force was generated on the skin's surface, which contributed to the development of MDRPU.

Disclosure Statement

All authors have no conflicts of interest to declare in this article.

Additional Statement

The content of this manuscript was presented at the 39th Annual Meeting of Japanese Society of Phlebology in 2019 in Nagoya, Japan.

Author Contributions

Study conception: KH
Data collection: all authors
Analysis: KH
Investigation: KH
Manuscript preparation: KH
Critical review and revision: all authors
Final approval of the article: all authors
Accountability for all aspects of the work: all authors

References

1) JSPU. Prevention and Management of Medical Device Related Pressure Ulcer. Tokyo: Shorinsha, 2016. (in Japanese)
2) National Pressure Ulcer Advisory Panel (NPUAP): NPUAP Pressure Injury Stages. NPUAP 2016. https://cdn.ymaws.com/npuap.site-ym.com/resource/resmgr/npuap_pressure_injury_stages.pdf (accessed 2019-07-05)
3) JSPU Survey Committee. Japanese Society of Pressure Ulcers survey report. Jpn J PU 2015; **17**: 141-58. (in Japanese)
4) JSPU Survey Committee. Japanese Society of Pressure Ulcers survey report 1. Jpn J PU 2018; **20**: 423-45. (in Japanese)
5) Zienkiewicz OC. The Finite Element Method. Yoshiki M, Yamada Y Trans. Tokyo: Baifukan, 1991.
6) Kuroda S, Akimoto M. Finite element analysis of undermining of pressure ulcer with a simple cylinder model. J Nippon Med Sch 2005; **72**: 174-8.
7) Linder-Ganz L, Shabshin N, Itzchak Y, et al. Assessment of mechanical condition in sub-dermal tissues during sitting: a combined experimental-MRI and finite element approach. J Biomech 2007; **40**: 1443-54.
8) Sari Y, Minematsu T, Huang L, et al. Establishment of a novel rat model for deep tissue injury deterioration. Int Wound J 2015; **12**: 202-9.
9) Linder-Ganz E, Gefen A. Mechanical compression-induced pressure sores in rat hindlimb: muscle stiffness, histology, and computational model. J Appl Physiol 2004; **96**: 2034-49.
10) Tamura Y, Takahashi M. Evaluation of antidecubitus cushion base on a finite element analysis of a 3-D buttock model. Transaction of JSMBE 2006; **44**: 598-605. (in Japanese)
11) Hashimoto K, Tosaki A, Matsuda N, et al. Observational study on efficacy in treatment by CDP based on severity of lymphatic function using elastic stockings and by LVSEA combined with pre-post operative the CDP for lymphedema. Jpn J Phlebol 2015; **26**: 236-43. (in Japanese)
12) Matsuda N, Tosaki A. Wear and removal of elastic compression stockings for lymphedema. Journal of Japanese Society of Limb Salvage & Podiatric Medicine 2016; **8**: 73-8. (in Japanese)
13) Hashimoto K, Tosaki A, Matsuda N. Consideration on the effectiveness of compression therapy with elastic stockings in intensive drainage treatment for lymphedema: from the perspective of interface pressure. Jpn J Phlebol 2018; **29**: 315-21. (in Japanese)
14) Matsuda N, Tosaki A, Hashimoto K. Devising ways to be negative interface pressure gradient when donning medical elastic stockings with graduated compression profile during an intensive drainage treatment for lymphedema: a successful case report. Jpn J Phlebol 2019; **30**: 267-71. (in Japanese)
15) Hashimoto K, Tosaki A, Matsuda N. Study on an improvement in sclerosis of skin by wearing a garment made of corrugated urethane sheet for lymphedema—numerical analysis by two-dimensional mechanical model—. Japanese Journal of Lymphology 2017; **40**: 31-7. (in Japanese)
16) Hirai M, Maki A, Hayakawa N. Clinical significance of double stockings in treatment of venous insufficiency. Journal of Japanese College of Angiology 1998; **38**: 57-61. (in Japanese)
17) Partsch H, Partsch B, Braun W. Interface pressure and stiffness of ready made compression stockings: comparison of in vivo and in vitro measurements. J Vasc Surg 2006; **44**: 809-14.
18) RIKEN Mechanical Property Database 2008; http://cfd-duo.riken.go.jp/cbms-mp/jndex.htm (accessed 2018-10-22)
19) Thomas S. The use of the Laplace equation in the calculation of sub-bandage pressure. EWMA Journal 2003; **3**: 21-3.
20) Nakai Z, Mimura K, Sakagami T. Mechanics of Materials. Tokyo: Asakura Publishing 2013: 119-21. (in Japanese)
21) Bader DL, Barnhill RL, Ryan TJ. Effect of externally applied skin surface forces on tissue vasculature. Arch Phys Med Rehabil 1986; **67**: 807-11.
22) Bennett L, Kavner D, Lee BK, et al. Shear vs pressure as causative factors in skin blood flow occlusion. Arch Phys Med Rehabil 1979; **60**: 309-14.
23) Kayama M, Koyama H, Yamamoto S, et al. Development of a pressure and shear force generating system and its analysis for discuss of mechanism of pressure ulcers. Proceedings, JSME Conference on Welfare, wellbeing, life support 2010: 461-2. (in Japanese)
24) Shimizu N, Komeda T, Koyama H, et al. Research on mechanism analysis for pressure ulcers. Proceedings, JSME Conference on Bioengineering 2009: 491-2. (in Japanese)
25) Yamamoto Y, Doi Y, Akiyama Y, et al. Biomechanical simulation for prevention of pressure ulcers (1. FEM simulation). Transaction of JSMBE 2008; **46**: 489-94. (in Japanese)
26) Stekelenburg A, Strijkers GJ, Parusel H, et al. Role of ischemia and deformation in the onset of compression-induced deep tissue injury: MRI-based studies in a rat model. J Appl Physiol 2007; **102**: 2002-11.
27) Carvile K, Lewin G, Newall N, et al. STAR a consensus for skin tear classification. Primary Intention 2007; **15**: 18-28.
28) Murasawa Y, Nemoto T, Isogai Z, et al. Valuation of dermal connective tissue under the loading of mechanical damage. JSME Proceedings, Yamanashi district conference 2016; 171-2. (in Japanese)
29) JSPU Survey Committee. Japanese Society of Pressure Ulcers survey report 3. Jpn J PU 2018; **20**: 486-502. (in Japanese)